Natural Hazards 1 (1988) 67–96.

Seismic Parameters Controlling Far-field Tsunami Amplitudes: A Review

EMILE A. OKAL
Department of Geological Sciences, Northwestern University, Evanston, IL 60208, U.S.A.

(Received: 13 July 1987; revised: 11 December 1987)

Abstract. We present a review of the influence of various parameters of the sources of major oceanic earthquakes on the amplitude of tsunamis at transoceanic distances. We base our computations on the normal mode formalism, applied to realistic Earth models, but interpret our principal results in the simpler framework of Haskell theory in the case of a water layer over a Poisson half-space. Our results show that source depth and focal geometry play only a limited role in controlling the amplitude of the tsunami; their combined influence reaches at most 1 order of magnitude down to a depth of 150 km into the hard rock. More important are the effects of directivity due to rupture propagation along the fault, which for large earthquakes can result in a ten-fold decrease in tsunami amplitude by destructive interference, and the possibility of enhanced tsunami excitation in material with weaker elastic properties, such as sedimentary layers. Modelling of the so-called 'tsunami earthquakes' suggests that an event for which 10% of the moment release takes place in sediments generates a tsunami 10 times larger than its seismic moment would suggest. We also investigate the properties of non-double couple sources and find that their relative excitation of tsunamis and Rayleigh waves is in general comparable to that of regular seismic sources. In particular, landslides involving weak sediments could result in very large tsunamis. Finally, we emphasize that the final amplitude at a receiving shore can be strongly affected by focusing and defocusing effects, due to variations in bathymetry along the path of the tsunami.

Key words. Tsunami excitation, seismic sources, tsunami earthquakes.

1. Introduction

The purpose of this paper is to present a general review of the seismic factors contributing to the far-field amplitude of a transoceanic tsunami. It has long been known that the final amplitude of a tsunami wave at a coastal station is a combination of the amplitude of the tsunami on the high seas, and of the response of the coastal area to the wave, the latter itself a combination of the so-called 'run-up' expressing the increase in wave amplitude upon shoaling, and of the response of any particular bay or harbor. Given an adequate modeling of coastal and harbor bathymetry, these effects can be successfully computed through numerical techniques such as finite element or finite difference codes (e.g., Iida *et al.*, 1983; Raichlen *et al.*, 1983); however, in order to predict the final amplitude of the waves, such methods require the knowledge of the amplitude on the high seas, which in effect constitutes an initial condition (both in space and time) for the integration. Extensive investigations, both observational and computational, generally suggest that run-up and resonance can increase a tsunami wave by a factor of 2 to 20 (e.g., Hwang and Lin, 1970). The

present paper will not discuss the response of a shoreline to tsunamis, but rather focus on the relationship existing between the tsunami wavefield on the high seas, typically several thousands of km away from its epicenter, and the seismic characteristics of the source.

1.1. *Physical Representation of Tsunami Sources*

Tsunamis are generated in oceanic areas by sources associated with catastrophic geophysical events, such as earthquakes, landslides and certain volcanic phenomena. Various systems of body force equivalents have been used to describe these sources.

- *Earthquakes* have generally been modeled successfully as double couples, whose mathematical representation consists of a purely deviatoric moment tensor. We refer to Aki and Richards (1980, p. 117) for a description of the relationship between the various tensor elements and the orientation of the fault plane and slip. The Chilean earthquake of 1960 is the most recent example of a catastrophic, Pacific-wide earthquake-generated tsunami.
- *Submarine landslides* have become the focus of substantial interest since Kanamori and Given (1982) analyzed the seismic signature of the series of events accompanying the 1980 explosion of Mount St. Helens, and concluded that the landslide could be modeled as a long-period single horizontal force. Since then, Kanamori (1985) and Eissler and Kanamori (1987) have proposed to use a single force source to model the 1 April 1946 Aleutian event, and in the mechanism of the 29 November 1975 Kalapana, Hawaii earthquake. The 1946 event produced the strongest tsunami recorded in the Pacific in this century; the Kalapana event generated a substantial local tsunami.
- *Marine volcanic eruptions* and associated phenomena can be of very complex nature, and still lack adequate physical descriptions. For the explosion of Krakatoa in 1883, which generated what may have been the most catastrophic tsunami in recent history, there exists a satisfactory modeling of its air waves with the source taken as an atmospheric explosion (Harkrider and Press, 1967), but the tsunami has not been modeled directly. In the case of the Tori-Shima event of 13 June 1984, and on the basis of moment tensor inversion of seismic waves, Kanamori *et al.* (1986) have proposed to invoke a contained magma injection followed by magma-water interaction, and to describe the source mathematically as a compensated linear vector dipole. In the case of the 1986 eruption of Mount St. Augustine Volcano, Kienle *et al.* (1987) have recently used finite different techniques to model the local tsunami as primarily due to the effect of the landslide accompanying the eruption.

1.2. *The Case of 'Tsunami Earthquakes'*

In the case of earthquakes, Kanamori (1972) and Abe (1973) pointed out early on that the amplitude of the tsunami is, in general, linearly related to the seismic moment M_0,

characteristic of the behavior of the seismic source at extremely long periods. However, Kanamori (1972) and later Fukao (1979) have pointed out to the so-called 'tsunami earthquakes', whose tsunamis are significantly larger (typically by a factor of 5–10) than would be predicted on the basis of their seismic waves. Examples include the 20 October 1963 Kurile Islands aftershock, the 10 June 1975 Nemuro–Oki earthquake, and the 19 December 1982 event in Tonga.

In the present paper, while reviewing the influence of various seismic parameters on tsunami excitation, one of our purposes will be to identify factors contributing to making a particular event a 'tsunami earthquake'.

2. Tsunami Theories

A tsunami consists of a gravity wave in which kinetic energy, due to laminar flow in the ocean column, is exchanged with gravitational energy, due to the motion of the water particles in the Earth's gravity field. In all practical examples in the Earth's ocean, elastic energy in the ocean column is negligible. There exist mainly two theories describing tsunami propagation and excitation:

2.1. *The Gravity Wave Theory*

In its simplest form, it considers the system of an incompressible oceanic layer of thickness H and density ϱ over a perfectly rigid half-space. The phase velocity of the wave, $C = \sqrt{(g/k)\tanh(kH)}$ is approximately $\sqrt{gH}$ in the long-wavelength limit $kH \ll 1$, where k is the wavenumber. We refer to Ben-Menahem and Singh (1981, pp. 790–796) for a detailed description of this theory. For our purposes, we will simply recall the following expressions of its solution:

$$\begin{aligned} y_1 &= Y(1 - z/H)\exp i(\omega t - kx), \\ y_2 &= -Y\varrho g z/H \exp i(\omega t - kx), \\ y_3^* &= -i(Y/kH)\exp i(\omega t - kx), \\ y_5 &= Y4\pi\varrho G(H - z)\exp i(\omega t - kx), \end{aligned} \tag{1}$$

where Y is a normalizing constant (which we will take as unity from now on); y_1 and y_3^* are the vertical and horizontal components of displacement, respectively; $-y_2$ is the local change in pressure, and y_5 the local change in gravity potential; z is the vertical coordinate, oriented positive downwards. These expressions are adapted from a previous study (Okal, 1982a; hereafter Paper I). It is particularly interesting to note that in the long-wavelength limit, most of the kinetic energy comes from the horizontal slushing of the water column, rather than from its vertical motion. Figure 1 illustrates the structure of the tsunami wave inside the oceanic column.

In this theory, the computation of the excitation of a tsunami wave by an underwater earthquake proceeds through the following steps: (1) use a realistic model (with finite elasticity) of the ocean floor and crust and compute the vertical component of the

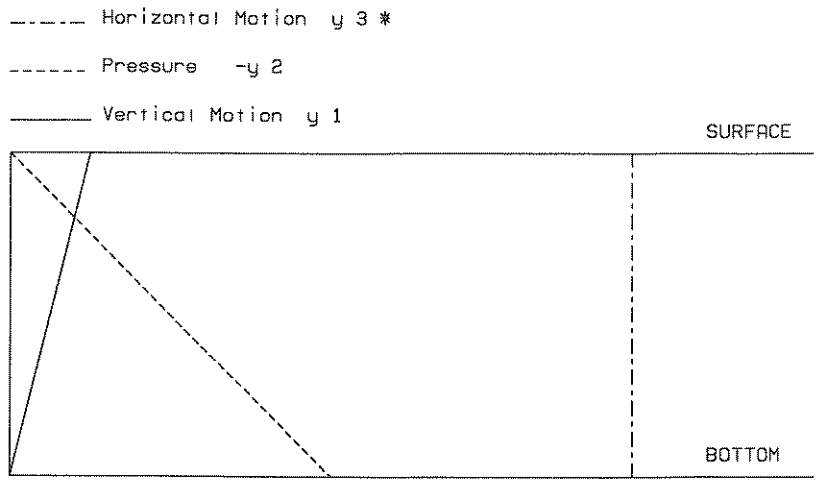

Fig. 1. Structure of a tsunami wave in the gravity wave formalism. The same scale is used for the horizontal and vertical components of motion, under the assumptions $H = 4$ km; $T = 1000$ s.

strong-motion displacement field $\mathbf{u}(x, y; t)$ on the ocean floor, (ii) use this expression of the strong-motion as a boundary condition in the general problem of the tsunami wave, expressing sudden (or almost sudden) deformation of the ocean floor (e.g., Ben-Menahem and Rosenman, 1972).

There are several problems with this approach: one of them is that the assumptions made in the two parts of its computation regarding the ocean floor are contradictory (elastic *vs.* rigid), precluding the correct modelling of any coupling effects between ocean and solid Earth, such as possibly induced by sedimentary layering. Also, the correct calculation of the tsunami excitation requires the accurate knowledge of $\mathbf{u}$ over an area of large dimensions, by seismic standards (typically on the order of the tsunami wavelength; $\Lambda \approx 300$ km), thus requiring extensive strong-motion calculations.

2.2. *The Normal Mode Theory*

This theory, introduced by Ward (1980), considers tsunamis as free oscillations of a self-gravitating Earth whose outermost shell is an ocean of thickness H. Major advantages of this approach include (i) the possibility of using a realistic model of Earth structure below the ocean, including an adequate description of sedimentary layering; (ii) the possibility of studying excitation readily through the use of the familiar normal mode excitation coefficients; and (iii) the automatic integration of the strong-motion of the water-rock interface over both time and the entire ocean floor. Finally, normal mode theory is well known to work best at long wavelengths and periods, clearly the domain of tsunami waves.

In Paper I, we proved theoretically the asymptotic equivalence of the two methods, and the existence of only *one* branch of tsunami modes. We also showed that neither the finite compressibility of water, nor the finite rigidity of the ocean's floor, affect

significantly the dispersion $C = \sqrt{gH}$ of tsunami modes in the long-wavelength approximation. As pointed out by Ward (1980), tsunami excitation by underground sources can be perceived as the excitation of the continuation of the eigenfunction into the solid Earth. Because this continuation is of very small amplitude, very large earthquake sources are required for tsunami excitation. In practice, and in very rough numbers, an earthquake of moment $M_0 \geqslant 4 \times 10^{28}$ dyn-cm is required to generate at a trans-Pacific distance ($\Delta \geqslant 60°$) a tsunami of about 15 cm, which through run-up and resonance at selected shorelines, will reach the level of several meters necessary to wage substantial flooding and destruction.

The equivalence of the two methods in marigram synthesis is a mere expression of the familiar Kirchhoff formulation of Huygens' principle in optics, namely that any wavefield can be constructed by isolating a particular surface, in this case the ocean floor, and treating it as a field of secondary sources (e.g., Sommerfeld, 1964, p. 195). Comer (1982) has verified this equivalence on the basis of synthetic seismograms.

2.3. *The Tsunami Wave Inside the Earth*

In the following sections, we will try to explain in simple terms some of our most important results regarding tsunami excitation. For this purpose, we now give a detailed description of the tsunami eigenfunction in the presence of an ocean floor with finite rigidity. Specifically, and as in Section 4 of Paper I, we consider the problem of tsunami modes for an oceanic column of depth $H = 4$ km, overlying a homogeneous elastic Poisson half-space. Figure 2 sketches the behavior of the various eigenfunction components, as obtained from normal mode computations, and for a period T close to 1000 s. For y_1 and y_3^*, note the different scales in the water, and hard rock. We also show on this figure the respective contributions of gravitational and elastic energy to the potential energy of the mode, both in the water column, and in the solid Earth. As noted by Ward (1980), the tsunami wave has practically no elastic energy in the water column, and its continuation into the solid Earth has only limited gravitational energy. As such, the latter, which we will call a 'pseudo-Rayleigh' wave, possesses the basic structure of a Rayleigh wave, except for a different set of boundary conditions (at the ocean floor, only the shear stress y_4 must vanish). Inside the Earth, the compressional and shear potentials Φ and Ψ of the pseudo-Rayleigh wave decay with depth as $\exp(-az)$ and $\exp(-bz)$, respectively, where $a = k\sqrt{1 - \kappa^2/3}$, $b = k\sqrt{1 - \kappa^2}$, and $\kappa = C/\beta$ is the ratio of the tsunami's phase velocity to the Earth's shear wave velocity. In the case of a tsunami wave, $\kappa \approx 0.05$, so that $a \approx b \approx k$. Our computations show that the pressure at the bottom of the ocean, $-y_2$, is a robust parameter, which is not affected by the finite rigidity of the half-space, and keeps the hydrostatic value $\varrho_{sea} g$. The vertical displacement y_1 at the interface is then controlled by the impedance of the half-space,

$$Z = \frac{y_2}{y_1} = -\mu k \frac{(2 - \kappa^2)^2 - 4\sqrt{(1 - \kappa^2)(1 - \kappa^2/3)}}{\kappa^2 \sqrt{1 - \kappa^2/3}}. \tag{2}$$

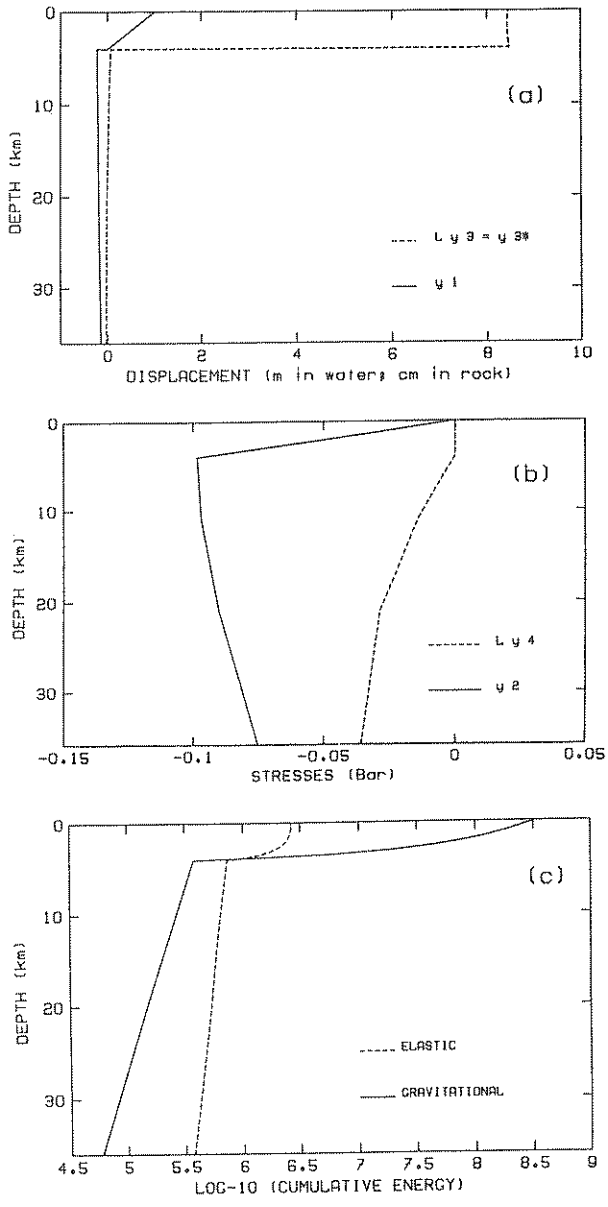

Fig. 2. Structure of a tsunami wave and of its continuation into the hard rock, in the formalism of normal mode theory (a): Eigendisplacements; note that the amplitude has been exaggerated 100 times for both y_1 and ly_3 in the rock, hence the apparent discontinuity in y_1. (b). Stresses y_2 and ly_4; the scale has *not* been changed in the hard rock; the scaling corresponds to an amplitude $y_1 = 1$ m at the surface. (c): Cumulative energy, integrated from the center of the Earth to a variable depth. Energy scale is logarithmic. Note that the gravitational energy in the water is about 10^4 times the elastic one, and 10^6 times the gravitational energy in the rock.

(The sign in this equation stems from the conventions of normal mode theory: y_1 positive upwards; y_2 positive for a tensional stress.) The vertical eigenfunction y_1 in the oceanic column is then adapted from the case of a rigid bottom to match its value $(-\varrho_{sea} g/Z)$ resulting from (2) at the bottom, rather than zero. In practice, and for typical values of C and β, one can take $\kappa \to 0$; then $Z \to \frac{4}{3}\mu k \gg \varrho_{sea} g$, so that the ratio of the amplitudes of y_1 at the surface and bottom of the ocean remains extremely large (typically on the order of 400), and the basic properties of the tsunami wave in the oceanic column are unchanged. This result actually allows the two-step computation of tsunami excitation in the gravity wave theory.

3. Source Effects

In this section, we describe the influence on tsunami excitation of a large number of parameters, such as moment M_0, depth of source h, depth of the oceanic column H, focal mechanism of the source and azimuth to the station, length of rupture L. In a series of papers, Ward (1980, 1981, 1982a, b) investigated many of these aspects. The present discussion is largely based on his formalism, but provides a somewhat more complete review; in particular, we stress the influence of the azimuthally isotropic term characteristic of dipping fault planes, and corresponding to the moment tensor component M_{zz}; also, we look at a considerably wider range of source depths, extending our investigation down to 250 km.

In the formalism of Kanamori and Stewart (1976) for normal mode excitation and seismogram synthesis, the amplitude of the wave is directly proportional to

$$M_0 \frac{1}{U} [K_0 s_R - ilK_1 q_R - l^2 K_2 p_R]. \tag{3}$$

We refer to these authors' work for the exact expression of the excitation coefficients K_i, $i = 0, 1, 2$, and of the geometric coefficients p_R, q_R, s_R depending on the orientation of the double-couple at the source and on the azimuth of observation; l is the angular order of the normal mode, related to the wavelength of the tsunami through $\Lambda = 2\pi a/(l + \frac{1}{2})$, where a is the Earth's radius, and U the group velocity, which for tsunami waves in the long-wavelength approximation, is equal to C. In the present work, we will use three basic seismic geometries: a strike-slip earthquake on a vertical fault (SS; involving only K_2), a dip-slip earthquake on a vertical fault (DS; involving only K_1), and pure thrusting on a 45°-dipping plane (T45; involving both K_0 and K_2). These mechanisms are sketched on Figure 3. Any other double-couple mechanism can be obtained as a linear superposition of such mechanisms. We use an Earth model inspired from 1066A (Gilbert and Dziewonski, 1975), and featuring a 4 km deep ocean, overlying a 7 km crust with oceanic characteristics.

Figure 4 is an example of a marigram computed by normal mode summation for the T45 mechanism, at a distance of 40° ($\simeq$4500 km), and a source depth of 10 km. A moment of 10^{27} dyn-cm has been assumed. The marigram represents the vertical

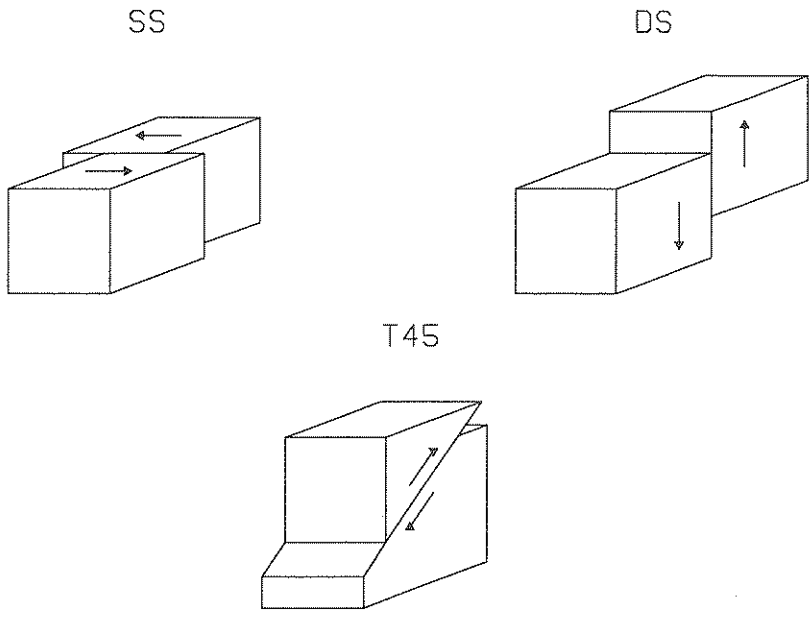

Fig. 3. Sketches of the geometry of rupture for the simple mechanisms SS, DS, and T45 investigated in this study.

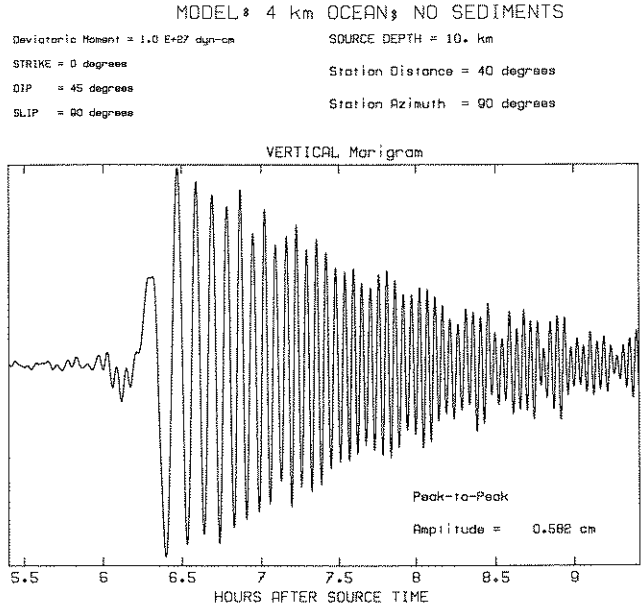

Fig. 4. Examples of marigram computed by normal mode summation for a thrust faulting event at a depth $h = 10$ km.

motion of the surface of the sea. It should be recalled that the horizontal motion of the sea will be about 10 times larger, according to (1).

3.1. *Seismic Moment*

As long as the tsunami wave can be considered as the superposition of the free oscillations of an elastic self-gravitating Earth, excited by a point source moment tensor, its amplitude should be directly proportional to the seismic moment M_0 of the earthquake. A number of studies (Abe, 1972) have shown a direct relationship between M_0 and tsunami amplitude; indeed Abe (1979) has used tsunami height records in Japan to infer moments for historical earthquakes predating seismic instrumentation. Figure 5 compiles the heights of 15 tsunamis recorded at Papeete, Tahiti. Our experience has shown that this location has the property of minimizing run-up and resonance effects. The tsunami amplitudes are compared to the earthquakes' seismic moments M_0, as available in the literature, after correcting by a factor $\sqrt{\sin \Delta}$ to account for the geometrical spreading on the spherical surface of the Earth. In general, it is seen that a direct linear relationship between tsunami amplitude and seismic moment holds over three orders of magnitude; however, there exist clear deviations from it: Both the 1960 Chile and 1964 Alaska events have deficient tsunamis; we will show that these can be explained as due to directivity and path effects. The

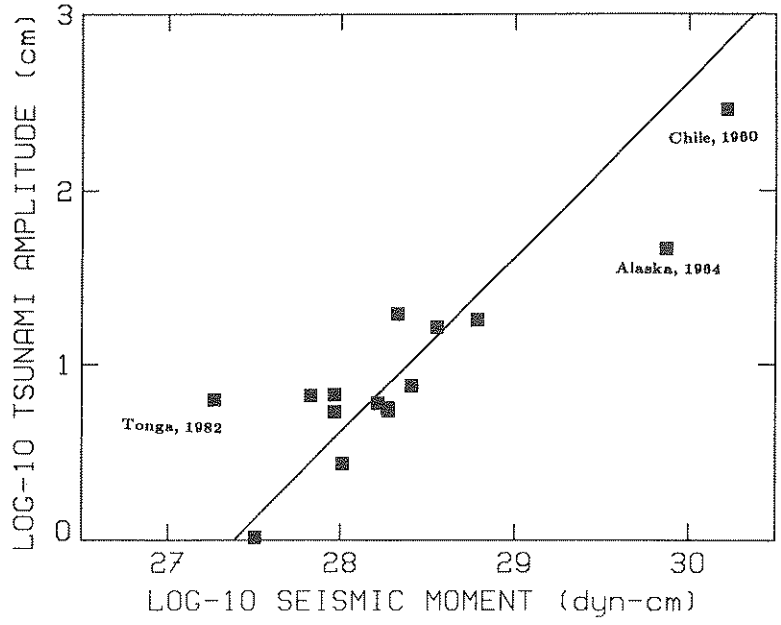

Fig. 5. Correlation between the amplitude of 15 tsunamis recorded at Papeete and the seismic moment of the parent earthquake. The amplitudes have been corrected by a factor $\sqrt{\sin \Delta}$ to account for geometrical spreading on the Earth. Note that the 1960 Chile and 1964 Alaska tsunamis are deficient (respectively because of defocusing and directivity), while the 1982 Tonga event would qualify as a 'tsunami earthquake'.

1982 Tonga event on the other hand has a tsunami about 10 times larger than expected from its moment; it would qualify as a 'tsunami earthquake'.

Abe (1979, 1983) has introduced a new tsunami magnitude M_t, directly proportional to the logarithm of the tsunami amplitude, and observed empirically an excellent correlation between M_t and the 'moment' magnitude M_w introduced by Kanamori (1977). This is in contradiction to our results, since M_w is proportional to $\frac{2}{3}\log_{10} M_0$. However, this may be an artifact of directivity effects for very large events, as discussed more in detail in Section 3.7 below.

Finally, Comer (1980) has argued that a linear relationship between tsunami amplitude and seismic moment can be expected only in the case of the so-called highly dispersive propagation. His model, which considers an extended source will also be discussed more in detail in Section 3.7.

3.2. *Radiation Pattern*

Tsunami radiation from a point source follows the general pattern of other seismic surface waves. Pure SS sources produce four-lobe clover-leaf patterns with maximum radiation at azimuths 45° from the strike of the fault; DS sources have two-lobe radiation patterns with maxima at right-angles from the strike of the fault. In the case of thrust faulting, the shape of the radiation pattern should depend *a priori* on depth and frequency; the general expression of the excitation is proportional to $[K_0 s_R - l^2 K_2 p_R]$, or in the case of the T45 mechanism ($s_R = 0.5; p_R = -s_R \cos 2\phi$), to $[K_0 + l^2 K_2 \cos 2\phi]$, with K_2 and K_0 proportional to $y_3(r_s)$ and

$$\frac{2(3\lambda_s + 2\mu_s)}{\lambda_s + 2\mu_s}\left[y_1(r_s) - \frac{r_s}{3\lambda_s + 2\mu_s} y_2(r_s) - \frac{l(l+1)}{2} y_3(r_s)\right], \tag{4}$$

respectively (Kanamori and Cipar, 1974). In this Equation, λ_s and μ_s are the Lamé coefficients at the source, and r_s the distance from the source to the center of the Earth.

For the standard Rayleigh wave of a homogeneous Poisson Earth, in a range of wavelengths Λ such that $h \ll \Lambda \ll a$, where a is the Earth's radius, and in the limit of shallow sources, y_2 vanishes at the source, and the ratio $y_3^*/y_1 = l y_3/y_1$ approaches -0.68. Thus only the third term in K_0 is relevant, and the ratio K_0/l^2K_2 approaches $-\frac{5}{3}$. The radiation pattern $(-\frac{5}{3} + \cos 2\phi)$ is the familiar potato-shaped one, with a ratio of four between its maxima and minima of amplitude (see Figure 6a).

In the case of a tsunami wave, and for the Poisson half-space considered in Section 2.3, the ratio y_3^*/y_1 at the ocean's bottom is expected to become:

$$y_3^*/y_1 = \frac{(2-\kappa^2) - 2\sqrt{(1-\kappa^2)(1-\kappa^2/3)}}{\kappa^2\sqrt{1-\kappa^2/3}}; \tag{5}$$

y_2/y_1 itself is given by (2). In the limit $\kappa \to 0$, one has $y_2/y_1 \to \frac{4}{3}\mu k$ and $l y_3/y_1 \to 1/3$. Thus $K_0/l^2K_2 \to -\frac{1}{3}$ and the radiation pattern $(-\frac{1}{3} + \cos 2\phi)$ features a ratio of only 1.6 between its maximum and minimum of amplitude (see Figure 6b).

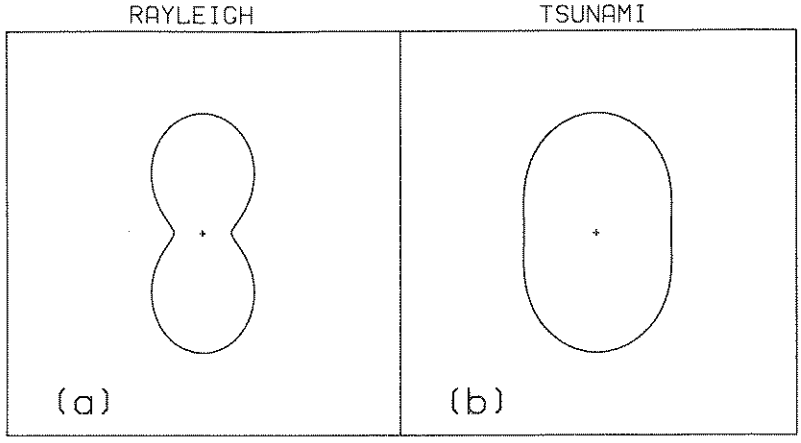

Fig. 6. Theoretical radiation patterns for Rayleigh waves (a) and tsunamis (b), for a Poisson half-space, a shallow source, and in the low-frequency limit. The two scales are unrelated. In both cases, the strike of faulting is oriented from left to right.

Therefore, in the long wavelength limit and for a homogeneous Poisson substratum, the tsunami radiation pattern of a T45 point source is more isotropic than that of a standard Rayleigh wave. However, in the more general case of a layered substratum, there can be a difference for shallow sources between the rigidity at the source (μ_s) and the average rigidity controlling the impedance Z of the solid medium, and the general shape of the radiation pattern of the T45 mechanism can then be expected to vary significantly.

In order to study systematically the influence of depth and focal mechanism, we computed marigram synthetics at a common distance of 40°, for the three basic sources, SS, DS, and T45, at many depths ranging from 100 m into the solid rock to 250 km. Figure 7 is a compilation of the peak-to-peak amplitude of such marigrams. For the two 'pure mechanisms', the synthetics were computed in the azimuth of the maximum of the radiation pattern (45° from the SS fault, and 90° away from the DS one). For the T45 mechanism, and given the above remark, we computed tsunami amplitudes at incremental azimuths of 10°, and for all depths kept the largest value (usually along strike at crustal depths, 90° from strike for mantle sources).

3.3 *Depth: A Minor Influence*

Perhaps the most important result of this study is the fact that depth of source plays only a minor role in the excitation of tsunamis. Figure 7 shows that the amplitude of a teleseismic tsunami is only reduced by a factor of 2 when depth varies between 20 and 100 km. The rapid variation with depth noted by Ward (1980) in the shallowest parts of the solid Earth is reproduced here, but slows down considerably (or can even be reversed) at greater depths. This can be attributed to the change of structural properties between crust and mantle. Most intuitive reasoning (occasionally found in

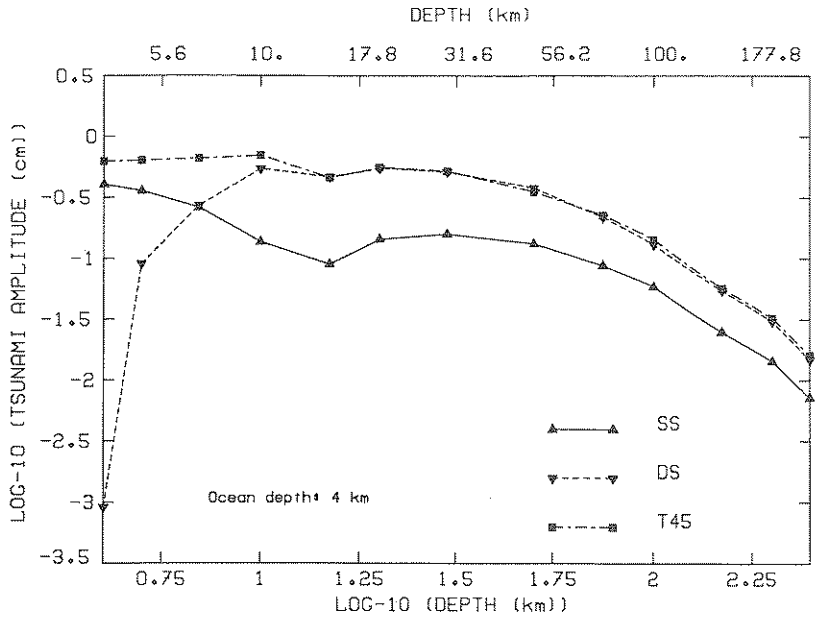

Fig. 7. Tsunami excitation as a function of depth and focal mechanism for a 4-km ocean model. These curves represent the peak-to-peak amplitudes of synthetic marigrams at a distance of 40° from the source, and in the direction of maximum radiation (see text for details). Various lines and symbols identify the three sources used.

the literature) would hold that only very shallow events are capable of tsunamigenic effects, an expression of the fact that the shallower the event, the larger the strong motion at the Earth's surface (or in the present case at the bottom of the ocean). Our investigation clearly points out to significant tsunami effects from earthquakes as deep as 100 km.

This apparent paradox can be understood in two ways. First, in the normal mode framework, one can study the structure of the pseudo-Rayleigh wave which continues the tsunami eigenfunction inside the Earth (see Section 2.3). Because the various components of the eigenfunction decay like $\exp(-az)$ or $\exp(-bz)$, with $a \approx b \approx k$, typically in the range $k \approx 2\pi/300\,\mathrm{km}^{-1}$, the excitation coefficients will themselves decay at this rate, and can remain significant in the first 100 km of the Earth. This is directly comparable to the decay of a standard Rayleigh wave with a wavelength approximately 2.5 times shorter (typically in the period range $T = 30$ s), whose shear potential Ψ is known to vary with depth as $\exp(-0.394\,kz)$; it is well-known that all earthquakes shallower than 100 km have substantial Rayleigh waves in this period range, and that it is necessary to move the source much deeper (e.g., beyond 200 km) before their excitation is reduced significantly.

In the formalism of the classic gravity wave theory, one must remember that a substantial tsunami will be generated only if a sufficiently large *volume* of water is displaced (in phase) by the motion of the ocean floor. Increasing the hypocentral

depth reduces the strong motion displacement at the ocean floor, but also increases the area over which this deformation takes place coherently, thereby reducing the destructive interference brought by integrating the source of the tsunami over the whole ocean floor.

An interesting illustration of the capacity of relatively deep events to generate substantial tsunamis is the modeling of the 22 June 1977 Tonga event. Several investigations (Talandier and Okal, 1979; Lundgren and Okal, in press) have indicated that this large earthquake ruptured the entire slab. Its moment has been estimated by Talandier and Okal (1979) as 1.5×10^{28} dyn-cm, while Silver and Jordan (1983) have found that it increases at low-frequencies to values as high as 2.5 and possibly 3 times 10^{28} dyn-cm. We model the source as a rupture propagating downwards from 50 to 162 km, along the steeply dipping fault plane (strike $\phi_f = 200°$; dip $\delta = 73°$; slip $\lambda = 297°$), and predict an amplitude of $\simeq 5$ cm at Tahiti. This is within a factor of 2 of the reported 10 cm. The most important aspect of this computation is that the amplitude of the tsunami created from this event with a hypocentroid located at 100 km depth, is reduced by only a factor of 4 from the case of a shallow event in the same geometry (see Figure 8). A notable difference is however the disappearance of the higher-frequency components of the tsunami wave, as noted earlier by Ward (1980).

3.4. *Focal Mechanism*

It is immediately apparent from the three curves on Figure 7 that the influence of focal mechanism on tsunami excitation is only marginal. In general DS and T45 mechanisms provide slightly greater excitation than SS. As expected, DS becomes very ineffective in the uppermost part of the crust, where the shear traction y_4, to which K_1 is directly proportional, must vanish at the ocean's bottom. In the same region, the most effective mechanism becomes the reverse fault (T45) characteristic of many subduction zone events. At depths of about 30 km, there is practically no difference in excitation between T45 and DS, a result already mentioned by Ward (1982b).

It is interesting to discuss these results in the framework of the classic gravity wave theory: while in the present section we keep the concept of a point source, it must be borne in mind that its effect must be integrated over the whole ocean floor to recover the tsunami field. As such, the shallow thrust fault mechanism is obviously superior in that it produces a large area of coherent uplift immediately over the hypocenter. On the other hand, the DS mechanism results in two regions of strong uplift and subsidence, separated by a characteristic distance going to zero with the depth of the seismic source into the hard rock; as this distance goes to zero, the phase lag between these two regions, considered as secondary Huygens sources, goes to π (as seen from any azimuth), and the surface integral of the deformation taken on the whole ocean floor vanishes.

Finally, we want to point out that focal mechanism alone cannot explain 'tsunami earthquakes'. It has been argued (Ward, 1982b) that the discrepancy between seismic

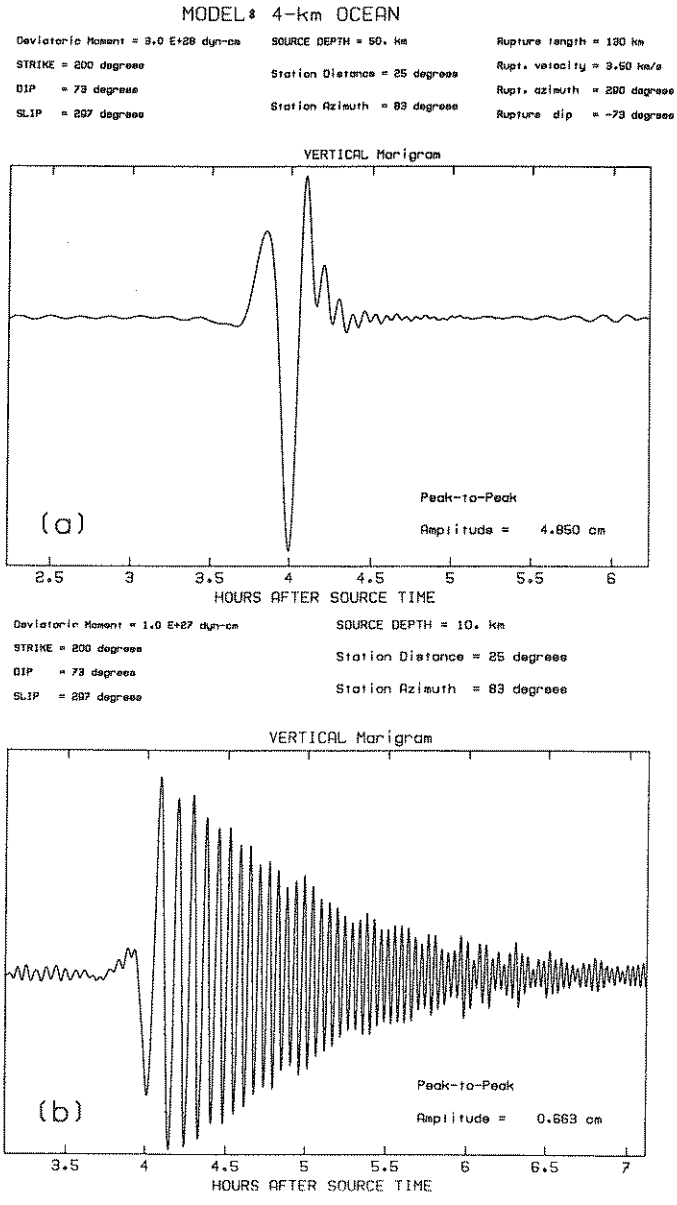

Fig. 8. (a): Synthetic marigram modelling the Tonga tsunami of 22 June 1977 at Tahiti. (b): Synthetic marigram for a shallow source (10 km) in the same geometry. Note that the deep-rupturing source generates less high-frequency, but that the amplitude remains about $\frac{1}{4}$ of that of the shallow source.

and tsunami excitation for such events could be due to mechanisms approaching the DS configuration, at very shallow depths. Under such geometry, the excitation of Rayleigh waves has long been known to be deficient. A seismic magnitude, or moment, computed under the assumption of the wrong focal mechanism could be

artificially small, and thus, the argument went, the tsunami's excitation enhanced with respect to seismic waves. It is clear that one has to be careful to take into account the fact that the shallow DS source is inefficient at exciting tsunamis for the exact same reason it does not excite surface waves: because the shear stress y_4 and thus also the coefficient K_1 must vanish at the ocean floor. For that purpose, Ward (1982b) introduces the concept of a 'skin depth' below which the boundary condition ceases to influence the DS excitation. It is easy to extend the concept a little further, and to compute an estimate of the depth at which K_1 will be a maximum. In the formalism of Section 2.3, y_4 behaves like $[\exp(-bz) - \exp(-az)]$, and is therefore maximum when $b/a = \exp(b - a)z$. For a Rayleigh wave in a Poisson half-space, for which $b = 0.394\,k$ and $a = 0.848\,k$, this yields $z = 0.27\,\Lambda$, where Λ is the wavelength; for the pseudo-Rayleigh wave continuing the tsunami, with $\kappa \to 0$, the solution is $z = 0.16\,\Lambda$ (typically 30 km). Ward's (1982b) argument is based on the use of very long period Rayleigh waves, for which the maximum DS excitation will occur around 220 km depth (typically, $\Lambda = 800$ km). However, 20 s Rayleigh waves ($\Lambda = 80$ km) will have a maximum DS excitation around 20 km into the hard rock. Actually, Figure 7 shows that the tsunami wave is excited significantly at depths shallower than predicted (this being due to the combined influence on y_4 of crustal layering, and of the coupling between the shear traction y_4 and the gravity terms ignored in our treatment of the continuation of the tsunami eigenfunction into the solid Earth); the point remains, however that while this theory predicts a disparity of excitation between the tsunami wave and very-long period Rayleigh waves for a shallow DS geometry, such disparity is largely absent if 20 s Rayleigh waves are considered. As such, Ward's (1982b) interpretation predicts that 'tsunami earthquakes' should also be characterized by a strong $M_s : M_0$ anomaly, i.e., a long-period moment *deficiency* as compared to their 20 s magnitude. This is not the case for either the 20 October 1963 Kurile aftershock, or the 10 June 1975 Nemuro-Oki event; actually the opposite is observed (Fukao, 1979). It is clear at this point that point source effects in homogeneous structures are not sufficient to account for 'tsunami earthquakes', and that a significant change in structure must be sought to further explain their characteristics. In Section 4, we will see that rupturing in a sedimentary layer can provide significant enhancement of tsunami excitation.

3.5. *Thickness of the Oceanic Column*

The influence of a change in the thickness H of the oceanic model can be investigated, once again, by reverting to the structure of the pseudo-Rayleigh wave described in Section 2.3: according to Equations (1), the depth of the water column does not affect the amplitude of the pressure wave $(-y_2)$ at the ocean's bottom, which itself controls the structure and amplitude of the pseudo-Rayleigh wave inside the solid Earth, through the impedance Z. In the long-wavelength limit, $(\kappa \to 0)$, Z is proportional to k, therefore to $H^{-1/2}$ for constant ω. Thus the displacements y_1 and y_3^* at the top of the substratum are proportional to $H^{1/2}$. The total energy of the tsunami wave can be

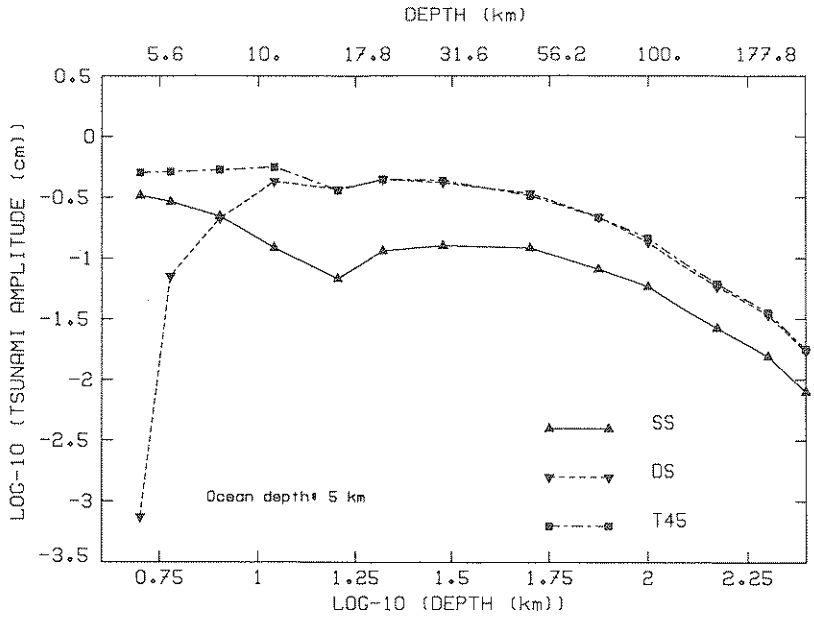

Fig. 9. Same as Figure 7 for a 5 km deep ocean. Note 20% decrease in excitation for shallow sources.

computed as the kinetic energy due to the horizontal slushing in the water column $\frac{1}{2}\int_0^H \omega^2 y_3^{*2}\,dz$. At a given frequency ω, and in the water column, $y_3^* \sim H^{-1/2}$, so that the energy of the wave is independent of H. As a result, and for shallow sources, because the eigenfunction in the solid Earth varies like $H^{1/2}$ and the energy integral is unchanged, the excitation coefficient K_2 varies like $H^{1/2}$. Since $U = C \sim H^{1/2}$, the spectral excitation (3) and eventually, the whole marigram are proportional to H^{-1}.

Figure 9, the equivalent of Figure 7 in the case of a 5 km ocean, confirms this result: for comparable shallow depths below the ocean's bottom, the amplitudes of the resulting tsunamis are diminished by a factor $\frac{5}{4}$, exactly inverse of the ratios of the ocean thicknesses. At substantially greater depths, this effect is reduced by the slower decay of exp $-kz$ and thus below 40 km, the influence of H is negligible.

These results are valid for oceans of homogeneous depth. In real life, if a tsunami is generated in an area of deep bathymetry (e.g., at an oceanic trench), the wave will be given an amplitude controlled by the corresponding excitation coefficients (i.e., inversely proportional to H). Its amplitude can later evolve, upon travelling into an oceanic basin with more different bathymetry. We should also keep in mind that H must be averaged over an area of dimensions comparable to Λ before the excitation is evaluated.

3.6. *Explosive Sources in the Water*

The normal mode formalism can readily be used to investigate the tsunami radiated by a large underwater explosion. Because the excitation coefficient N_0 for such a source is directly proportional to the dilatation, or pressure, field of the eigenfunction

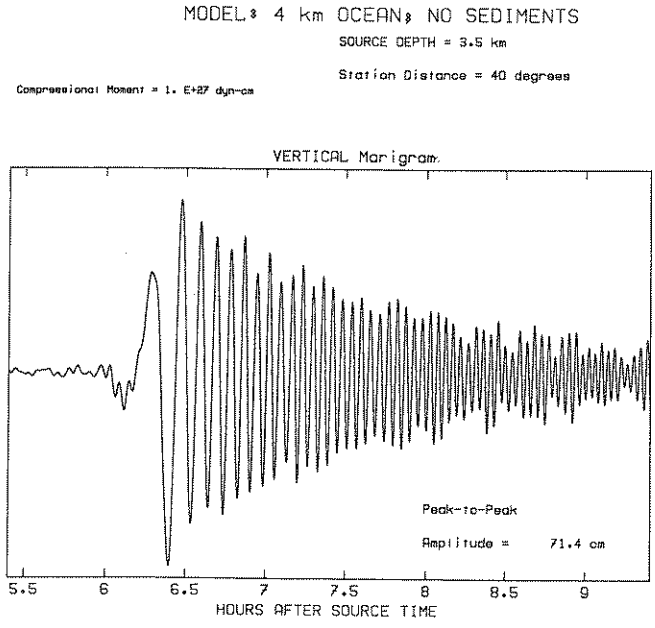

Fig. 10. Synthetic marigram for an explosion at a depth of 3.5 km in the water.

(Okal, 1978), the efficiency of such a source will be grossly linear with depth; our computations (see Figure 10) suggest that an explosive source of moment 10^{27} dyn-cm on the ocean's bottom will produce a tsunami of about 80 cm vertical amplitude at a distance of 40°. Conversely, a potentially catastrophic tsunami with an amplitude of 15 cm on the high seas would require an explosion with a seismic moment of 2×10^{26} on the ocean's bottom, or 1.5×10^{27} dyn-cm at a depth of 500 m. This is considerably larger than the largest known water explosion, 'WIGWAM', recorded 14 May 1955 with a moment of $\approx 10^{24}$ dyn-cm (E. A. Okal, unpublished data).

3.7. *Directivity Effects*

Up to now, we have considered only point sources. The very large earthquakes needed to generate significant tsunamis are characterized by rupture extending over very long faults (typically hundreds of km), and it has long been known that tsunamis are affected by extremely large directivity effects. As shown by Ben-Menahem and Rosenman (1972), the directivity function

$$D(\phi) = \operatorname{sinc}\left[\frac{\omega L}{2C}\left(\frac{C}{v_R} - \cos\phi\right)\right] \tag{6}$$

(where L is the length faulting, v_R the velocity of rupture, and ϕ the azimuth of observation relative to the direction of rupture) is maximum for $\phi = \cos^{-1}(C/v_R)$, which for tsunamis approaches 90°, since their phase velocity is typically ten times less than the rupture velocity at the source. The effect of $D(\phi)$ on the radiation pattern is,

in general, to narrow the lobes of the radiation pattern, and to produce additional lobes and nodes (Ben-Menahem and Rosenman, 1972; Ward, 1982b; Lynnes and Ruff, 1985). An alternate formalism is to keep the point source representation, but to include higher moments of the system of body forces, which are capable of exciting zonal harmonics of higher degrees (Okal, 1982b).

In the case of Pacific tsunamis, rupture along the major subduction zones is most often tangential to the oceanic basin, and thus the main lobes of the directivity patterns are straight into the center of the basin. Such Pacific islands as Hawaii, and French Polynesia, located roughly at the center of the Pacific basin, can expect to receive the full blow of a positive interference at the source. In this respect, the dataset presented on Figure 5, and with the exception of Alaska (see below), is probably more representative of the maximum amplitude Y of the tsunami than Abe's (1983) dataset, obtained at azimuths more scattered with respect to the directions of rupture. As a result, it is not surprising that our dataset supports a correlation of the type $Y \sim M_0 \sim L^3$, while Abe's, obtained in conditions where $D(\phi) \sim 1/L$, leads to $M_t = M_w \sim \frac{2}{3} \log_{10} M_0$, which is equivalent to $Y \sim L^2$.

A significant exception to this pattern was the 1964 Alaska earthquake, for which the azimuth of faulting is nearly radial to the Pacific basin, with most of the energy concentrated towards California and Chile (Ben-Menahem and Rosenman, 1972). In Table I we have used normal mode theory to compute synthetic marigrams at a number of Pacific stations selected for their relative insensitivity to run-up and resonance. The propagating source is modeled as a succession of 10 individual sources, adequately lagged in space and time. We used the following parameters (Kanamori, 1970) for the focal and rupture mechanism of the Alaskan event: source depth $h = 33$ km; moment $M_0 = 7.5 \times 10^{29}$ dyn-cm; fault strike $\phi_f = 246°$; dip $\delta = 20°$; slip $\lambda = 90°$; length of rupture $L = 600$ km; azimuth of rupture $\phi_R = 205°$; rupture velocity $v_R = 3.5$ km/s. The resulting directivity effect (defined as the ratio of amplitudes at right angles to, and along, strike) is about one order of magnitude; in particular, at Tahiti (azimuth $\phi_s = 183°$), the directivity factor $D(\phi)$ takes a value of 0.11, which is sufficient to fully explain the deficiency in tsunami amplitude for this event noted on Figure 5.

Similarly, we refer to Ward (1982b) for a satisfactory modeling of the 13 October 1963 Kurile Islands mainshock. The Kurile and Alaska earthquakes are the only true gigantic events having generated Pacific-wide tsunamis in the past 25 years.

Table I. Modeling of the 1964 Alaska tsunami

Shore	Peak-to-peak tsunami amplitude (cm)	
	Computed	Observed
No. California	191	210
Hawaii	58	65
Midway	34	30
Tahiti	43	45

Finally, it is worth discussing more in detail Comer's (1980) model of tsunami propagation under either dispersive or nondispersive limits. In order to violate the linear relation between tsunami amplitude (Y in our notation, H in his), and M_0, Comer needs to be in the so-called nondispersive range, i.e., close to the epicenter or in a geometry involving a very large characteristic dimension R for the source; his source has a Gaussian profile and axial symmetry, but zero rise time. As such, at all azimuths, he suffers a destructive interference $\exp[-\omega^2 R^2/4C^2]$. In practice, by considering an azimuthally symmetric source, he always positions himself in a region of destructive interference; realistic rupture models are clearly of a much more elongated nature (e.g., up to 1000 km for the 1960 Chilean event), which allows for constructive interference at right angles from their direction.

3.8. *Non-Double Couple Sources*

In this section, we investigate the excitation of tsunamis by non-double couple seismic sources, such as those proposed to model submarine landslides and certain volcanic phenomena.

In the case of the seismic event near Tori-Shima on 13 June 1984, the compensated linear vector dipole [CLVD] proposed by Kanamori *et al.* (1986) can be considered as the superposition of two T45 mechanisms, at right angle from each other: this produces a single component (M_{zz}) in the moment tensor. The radiation pattern of the tsunami is expected to be isotropic with the average amplitude for a T45 mechanism at the same depth; it is clear that this alone cannot explain a stronger than normal tsunami excitation.

In the case of landslides, such as the 1946 Aleutian event, a representation by a single force has been proposed (Kanamori, 1985). In the framework of normal mode theory, excitation coefficients are readily computed for a single point force $\mathbf{F}$ by substituting $\mathbf{F} \cdot \mathbf{u}_s$, where $\mathbf{u}_s$ is the mode's eigendisplacement for the familiar product $\mathbf{M}, \varepsilon_s$ where ε_s is the eigenstrain (Gilbert, 1970). In the case of spheroidal modes, the excitation (3) must be replaced by $[F_r C_0 - ilF_h C_1 \cos\phi]/U$, where

$$C_0 = \frac{-1}{2} r_s \left[\frac{K_0 - 2N_0}{6} + \frac{l(l+1)}{2} K_2 \right],$$

$$C_1 = \frac{-1}{2} r_s K_2. \tag{7}$$

F_r is the vertical component of the single force, $\mathbf{F}_h$ its horizontal component, and ϕ the angle between the direction of propagation and $\mathbf{F}_h$.

The ratio of the relative efficiency of a single force F and a T45 double couple M_0 at exciting any type of wave is given by

$$R = \frac{\text{average } \{C_0; lC_1\}}{\text{average } \{K_0; l^2 K_2\}} \frac{F}{M_0}. \tag{8}$$

The coefficients C_0 and C_1 are directly proportional to the vertical and horizontal eigenfunctions, y_1 and y_3, respectively. We have seen earlier that in the case of homogeneous Poisson substrata, $ly_3/y_1 \to -0.68$ for Rayleigh waves, and 1/3 for tsunami pseudo-Rayleigh waves at the top of the solid Earth, both numbers being of order 1. Thus, the terms C_0 and lC_1 are of the same order of magnitude; similarly, we have seen that $|K_0/l^2K_2|$ remains on the order of 13/3 for tsunamis and 5/3 for Rayleigh waves. Thus, Equations (7) and (8) predict that

$$R \approx \frac{1}{l}\frac{Fa}{M_0},$$

where a is the Earth's radius. In the case of a tsunami, a typical value of the angular order is $l = 200$; in the case of Rayleigh waves, l varies from 40 at long periods to 500 around 20 s. We conclude therefore that in the case of a simple Poisson half-space, a single force gives a ratio of tsunami to very-long period Rayleigh wave excitation about five times less efficient than a double-couple; this ratio reaches 1 for 20 s Rayleigh waves. Clearly, single force mechanisms alone cannot account for 'tsunami earthquakes'.

4. Influence of Sedimentary Layering

In this section, we investigate the effect of a layer of sediments featuring weak mechanical properties between the oceanic column and the hard rock, on the excitation of tsunamis by various seismic sources. In paper I, we proved, both on the basis of the actual computation of tsunami modes, and from a theoretical standpoint, that the introduction of such a layer did not affect the *dispersion* (i.e., the eigenfrequency) of the tsunami modes. We prove here that rupture into a sedimentary layer can increase considerably the tsunami excitation for any mechanism involving a component of thrust faulting.

We are motivated in this endeavor by qualitative remarks by Fukao (1979), who noticed that the location of several 'tsunami earthquakes' was in the immediate vicinity of the sedimentary wedge immediately arcwards of the Kurile trench, and trenchwards from the seismic belt. He suggested that sedimentary structures should provide amplification of the strong motion at the bottom of the ocean, and thus of the tsunami excitation.

We use a model featuring a 4-km deep ocean, and the same hard rock structure as our 5 km model used in Figure 9. In between, we use a 1 km layer of sediments, characterized by a density $\varrho = 1.52\,\mathrm{g/cm^3}$ and seismic velocities $\alpha = 2\,\mathrm{km/s}$; $\beta = 1.15\,\mathrm{km/s}$. We want to emphasize that this model is a theoretical one, whose purpose is merely to explore some physical aspects of the role of sediments in tsunami excitation. In particular, detailed oceanic models of sedimentary structure have evidenced strong gradients of seismic velocities, due to fast increases in the degree of consolidation and in particular very low shear velocities in the shallowest layers (Spudich and Orcutt, 1980). Note that in our model, the sedimentary layer is taken

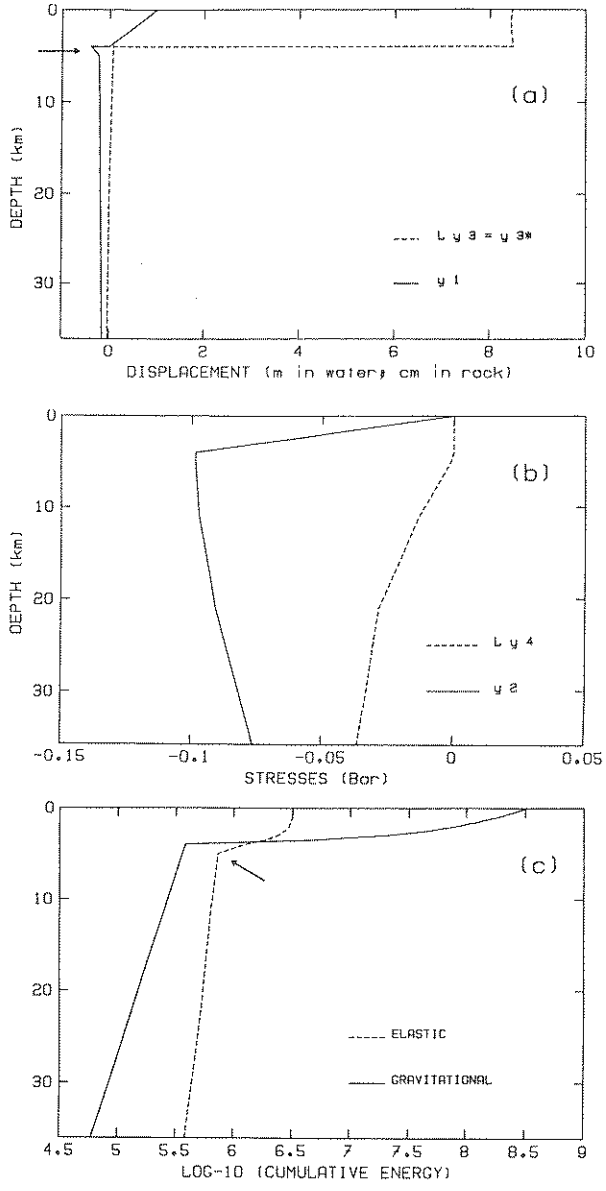

Fig. 11. Same as Figure 2 for a model incorporating a 1 km layer of sedimentary material. Note development of substantial y_1 in the sedimentary layer (arrow in (a)), build-up of elastic energy in the sedimentary layer (arrow on (c)), and absence of effect on y_2, y_3 and y_4.

as a Poisson solid, and its velocities could be characteristic of consolidated limestone. In this respect, this sedimentary model is not extreme; much 'looser' and weaker structures are encountered in Nature.

Figure 11 shows the behavior of the tsunami eigenfunction with depth in the presence of sediments. The effect of the inclusion of a sedimentary layer on the

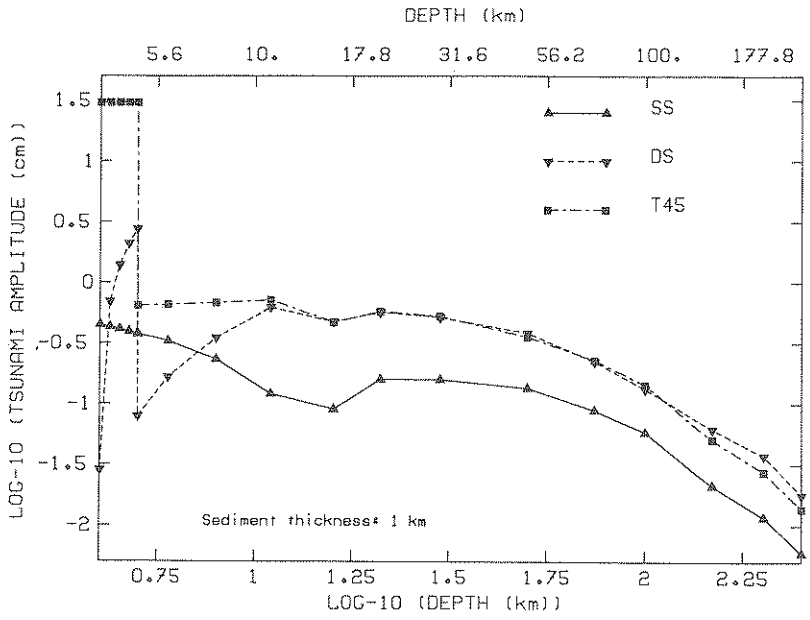

Fig. 12. Same as Figure 7 for a model incorporating a 1 km layer of sediments. Note significant increase in T45 excitation if the source is placed in the sedimentary layer.

excitation of tsunamis is shown on Figure 12. The latter can be summarized as follows: for a source placed inside the sedimentary layer, the T45 mechanism becomes about 100 times more efficient, the SS mechanism remains practically unaffected, and the DS excitation varies strongly throughout the layer, with an average excitation comparable to T45 outside the layer. No substantial changes are incurred if the source is left in the hard rock. The behavior of the gravity integrals confirms the change in excitation: inside the sedimentary layer, the elastic energy develops significantly (see arrow on Figure 11c), so that the wave can be excited by placing a source with adequate geometry inside the layer; on the other hand, in the solid rock, the elastic energy is basically unchanged.

This very large increase in the coefficient K_0 inside the sedimentary layer can be understood in the framework of the pseudo-Rayleigh wave described in Section 2.3. If we consider the simple model of a sedimentary layer over a half-space, it is possible to use a Haskell–Thomson propagator (Aki and Richards, 1980, p. 276) to compute the new impedance Z of the total medium consisting of sediments and half-space. The result is shown as the solid line on Figure 13. As expected Z is now a function of ω, but several points can be made. First, $Z = y_2/y_1$ is always smaller than its value $(\frac{4}{3}\mu k)$ in the absence of the layer; since the tsunami in the water column controls y_2 at its bottom, y_1 will be enhanced there and throughout the sediments. Second, at the sediment-hard rock interface, the impedance Z remains practically unchanged (as shown by the long dashes on Figure 13); also, the traction y_4 remains very small at the top of the hard rock (see short dashes on Figure 13), and the pressure $-y_2$ changes

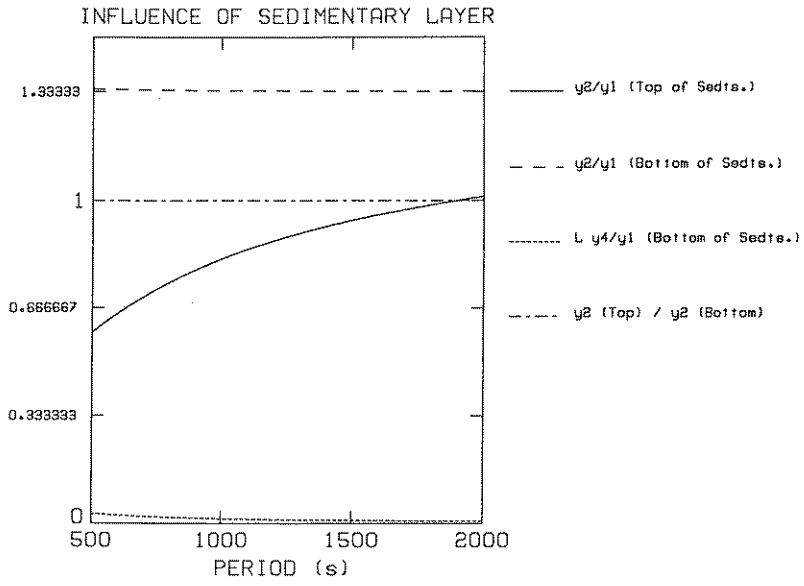

Fig. 13. Theoretical impedance of solid medium in the presence of sediments, computed from a Haskell–Thomson propagator, in the absence of water. Solid line: $Z(\omega) = y_2/y_1$ at top of sediments in units of μk, where μ is the rigidity of the hard rock; Large dashes: same at bottom of sediments; Short dashes: shear impedance ly_4/y_1 at bottom of sediments; Dash-dot line: ratio of y_2 at top and bottom of sediments.

very little throughout the sediments (dash-dot line on Figure 13). Finally, the vertical displacement y_1 at the ocean floor remains small compared to its value at the surface of the ocean (it is multiplied by no more than a factor of 2.5); as a consequence, the tsunami eigenfunction in the water should be left practically unchanged. Then the pressure at the top and bottom of the sediments is also unchanged from the model without sediments; since at the top of the hard rock, the shear traction remains practically zero, and the impedance Z also keeps its value, the pseudo-Rayleigh wave itself is unchanged inside the half space. These simple physical arguments, entirely based on the properties of the Haskell–Thomson propagator inside the sediments, readily explain that the hard rock excitation of the tsunami is unchanged. On the other hand, the larger value of y_1, and the lower values of λ and μ in the sediments act to boost K_0, according to Equation (4).

In contrast to the behavior of the tsunami wave continuation, standard Rayleigh waves ($T \geqslant 20$ s) are practically unaffected by the presence of sediments. Not only is their dispersion unchanged (which was expected due to the small ratio between the thickness of the layer and the wavelength), but the eigenfunction itself remains practically unchanged through the layer of sediments: our calculations indicate that even at 20 s, y_1 varies only a few percent between the ocean's surface and the base of the crust. y_2 remains very small both in the water and the sediments; under these conditions, the excitation coefficients, including K_0, remain on the same order of magnitude inside and outside the sediments.

4.1. *A Possible Model for 'Tsunami Earthquakes'*

The above remarks indicate a possible scenario for the development of a 'tsunami earthquake'. Figure 12 shows that a T45 source will be about 100 times more efficient at exciting a tsunami inside a sedimentary layer than in the hard rock, while its Rayleigh efficiency will be basically unchanged in the period range $T \geqslant 20$ s. While it is probably not feasible to envision a very large moment release, such as 10^{27} dyn-cm, in a sedimentary layer, we want to propose a model in which a shallow earthquake, rupturing all the way to the ocean floor sees *part* of its moment release take place inside the sedimentary layer. Specifically, we apply this model to the case of the two Nemuro-Oki earthquakes, studied by Fukao (1979): the 17 June 1973 regular event and the 10 June 1975 'tsunami earthquake'. Table II shows a list of parameters used in this experiment: the mechanism of the 1973 event is taken from Shimazaki (1975). Its rupture characteristics are taken under the simple assumption of an up-dip rupture. For the 1975 event, we keep the concept of a steeper dip and of a much shallower source (Fukao, 1979); we use a total rupture length of 50 km [assuming $M_0 \sim L^3$ scaling (e.g., Geller, 1976)], and an oblique direction of rupturing along the fault plane, allowing the rupture to reach the ocean floor (in practice, the last contribution to the source is taken at a depth of 100 m into the sedimentary layer). Figure 14 shows the resulting radiation patterns. It is remarkable that the two earthquakes have tsunamis of comparable amplitude, despite seismic moments in a ratio of about 8 to 1. Note that because the major contribution to the tsunami of the 1975 event is from the portion of moment release taking place in the sediments, through their K_0 term, the radiation pattern is practically azimuthally symmetric.

In conclusion, this crude model confirms rupturing into a material of weaker mechanical properties, such as a sedimentary layer, as a possible mechanism of 'tsunami earthquakes'. In this concept, a 'tsunami earthquake' is one for which a small (10%)

Table II. Parameters used in modeling Nemuro–Oki earthquakes

Parameter	Symbol	Value	
		17 June 1973 'Normal'	10 June 1975 'Tsunami earthquake'
Initial depth	h_0	48 km	10 km
Fault azimuth	ϕ_f	223°	223°
Fault dip	δ	22°	40°
Fault slip	λ	90°	90°
Rupture length	L	100 km	50 km
Rupture azimuth	ϕ_R	43°	43°
Rupture dip	δ_R	22°	6.7°
Rupture velocity	v_R	3.5 km/s	3.5 km/s
Seismic moment	M_0	6.7×10^{27} dyn-cm	8×10^{26} dyn-cm
Shallowest rupture beneath ocean floor		10.3 km (in hard rock)	0.1 km (in sediments)

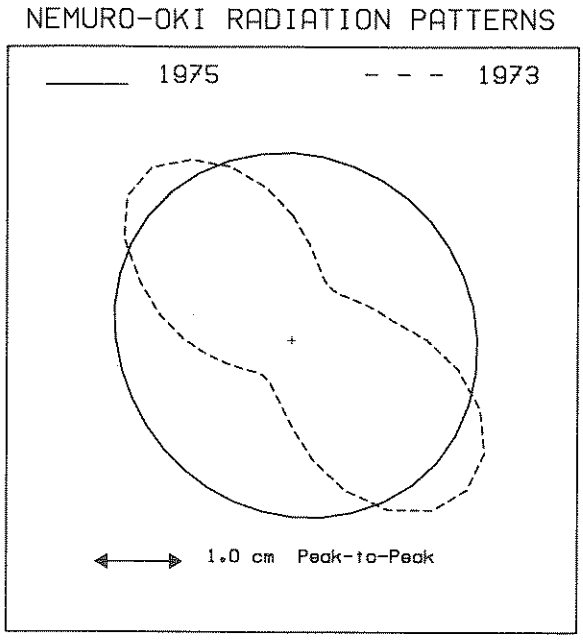

Fig. 14. Theoretical tsunami radiation patterns for the two Nemuro-Oki earthquakes of 1973 (dashed line) and 1975 (solid line), computed using parameters listed in Table II; note that the average amplitudes of the two tsunamis are comparable, despite moments in a ratio of 8:1.

fraction of the moment release takes place in the sediments. Although the earthquake may have a moment 10 times smaller than the 'regular' event, the increase in K_0 of about 100 assures tsunamis of comparable amplitude, these numbers being of course orders of magnitude.

We want to stress again that the mechanical properties of the sedimentary layer envisioned in this section are not extreme. Clearly, if one considers much looser material (known to exist in the first few meters of ocean floor), the strong motion under a large earthquake is expected to be highly non-linear, and the representation of the whole process by an equivalent moment tensor (or system of forces) in an elastic continuum may be inappropriate. However, for the relatively consolidated sedimentary structure involved here, the effects on tsunami excitation are sufficient to reach the order of magnitude of the anomalous behavior experienced during 'tsunami earthquakes'.

4.2. *The Case of Non-double Couple Sources in Sediments*

Finally, we explore the influence of a sedimentary layer on non-double couple sources. We first refer to the CLVD source proposed by Kanamori *et al.* (1986) for the presumed magma injection at Tori-Shima. Since this source corresponds to the superposition of two T45 mechanisms, its excitation is governed by the coefficient K_0;

tsunami excitation will be boosted significantly by placing it into weak material, while Rayleigh excitation will be largely unaffected.

In the case of the single forces used in modeling landslides, the situation is somewhat more complex. Our computations have shown that the introduction of a sedimentary layer affects y_3 and therefore K_2 significantly neither for a Rayleigh wave nor for a tsunami wave. Thus, the coefficients C_1 are not affected and the ratio of tsunami-to-Rayleigh excitation will remain relatively unchanged for a horizontal force. On the other hand, the increase in y_1 inside the sedimentary layer for the tsunami wave results in a similar increase in the coefficient C_0. A vertical force in sediments will excite tsunamis significantly better than Rayleigh waves.

Most modeling of landslides by single forces have resulted in a largely horizontal force. In the case of Mount St. Helens, Kanamori *et al.* (1984) have found that the vertical force, of much smaller amplitude and much shorter characteristic time, was due to the eruptive process itself. However, in the case of the submarine Kalapana event, Eissler and Kanamori (1987) have found a force oriented 10° on the horizontal, suggesting at least some component of vertical force. Also, we want to emphasize that the amplification of y_1 and consequently C_0 could become considerably stronger if the material properties of the sediments are further weakened. Thus it is possible that major submarine landslides involving some vertical forces could generate tsunamis significantly stronger than expected from their Rayleigh waves.

5. Path Effects

Finally, in this section, we want to point out to the importance of path effects on the final amplitude of a tsunami wave. On an ocean of homogeneous depth H, the phase velocity of the tsunami does not vary laterally, and its amplitude is expected to be controlled by geometrical spreading on a spherical surface:

$$Y \sim \frac{1}{\sqrt{\sin \Delta}}.$$

However, the depth to the ocean floor is known to vary substantially from shallow mid-oceanic ridges to deep oceanic basins, not to mention the existence of swells such as the Hawaiian chain or plateaux, such as the Tuamotu and Ontong–Java features. One therefore expects the velocity $\sqrt{gH}$ to vary significantly, in practice from 170 m/s to 230 m/s. Surface wave propagation in a field of heterogeneous phase velocities results in strong focusing and defocusing of the waves. In two recent studies, Woods and Okal (1987) and Satake (1988) have used ray-tracing to document such effects and have indicated on the basis of preliminary calculations that they can account for up to 1/2 order of magnitude towards the tsunami's amplitude. Figure 15 illustrates this concept. In particular, the deficiency in tsunami amplitude at Papeete from Chile (see Figure 5) can be explained at least in part by this mechanism.

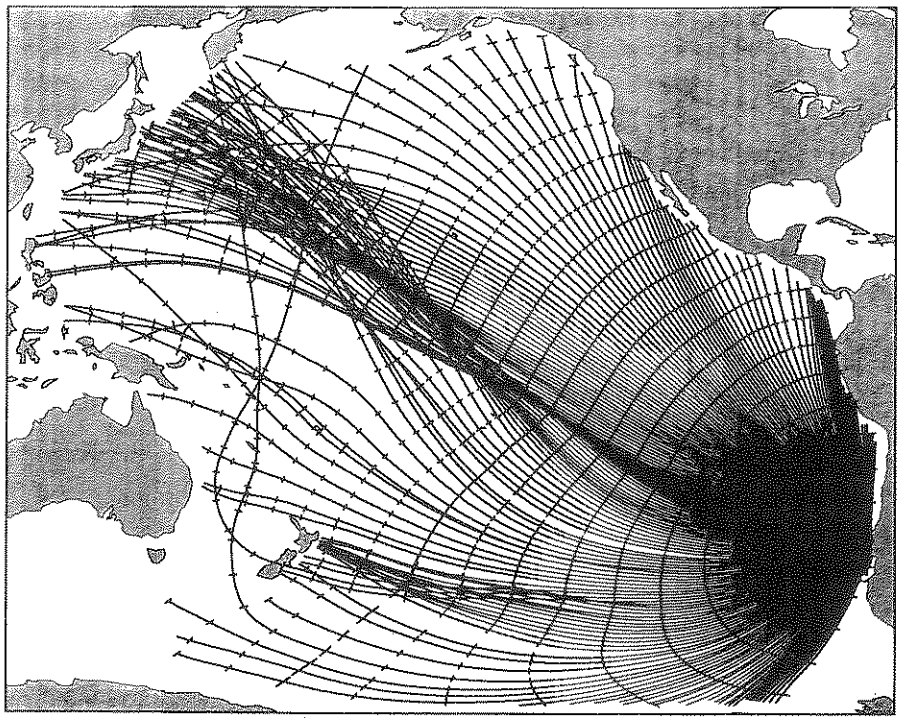

Fig. 15. Tsunami wave field resulting from ray-tracing for the 1960 Chilean earthquake (Woods and Okal, 1987). Rays are traced in 1° azimuth increments from the epicenter, and terminated upon reaching a continental shore. Tick marks show group times in increments of hours. Note strong focusing due to crossing the East Pacific Rise, and defocusing towards Alaska, the Aleutians and Polynesia.

6. Conclusions

In this paper, we have analyzed a large number of seismic parameters for influence in tsunami generation. In the general framework of tsunami warning, when a decision on issuing a watch and possibly evacuating low-lying areas must be made in a very short period of time, it is crucial to have a good understanding of the parameters whose influence is primordial.

- This study has clearly indicated that the primary parameter must be the seismic moment of the parental earthquake. Tsunami excitation grows in direct proportional relation to M_0. In this respect, recent efforts at obtaining a rapid estimate of M_0 are extremely important for tsunami warning (Okal and Talandier, 1987; Talandier *et al.*, 1987). The use of short-period seismic magnitudes which are known to saturate, such as the 20 s M_s or *a fortiori* the 1 s m_b, is to be proscribed for tsunami warning. A seismic moment of about 4×10^{28} dyn-cm is necessary to create a potentially destructive tsunami ocean-wide.
- On the other hand, depth and focal mechanism have little if any influence on tsunami excitation. Any large subduction zone event occurring in the first 100 to

150 km of the Earth is capable of generating a significant tsunami. Similarly, a variation in focal mechanism cannot account for more than about 0.5 orders of magnitude in the size of the tsunami. Solving for the event's focal mechanism and depth is probably not worth wasting the precious time separating the earthquake waves from the tsunami.

- Much more important is the effect of directivity at the source. While the rupture characteristics of an event are difficult to compute in real time, they can contribute one order of magnitude to the amplitude of the tsunami. Fortunately, this effect is always destructive, i.e., it always give rise to tsunami waves smaller if anything than expected from a point source of similar total moment. In addition, the orientation of rupture often can be tentatively estimated from the simple plate geography of the epicentral areas for most Pacific-rim earthquakes.
- Rupturing propagating into a sedimentary layer is believed to play a major role in the origin of the so-called 'tsunami earthquake'. Theoretical investigations indicate that the excitation of a tsunami by a thrust fault mechanism can gain 1 order of magnitude by just locating 10% of the moment release inside a layer of weaker mechanical properties. Fortunately, documented 'tsunami earthquakes' have usually taken the form of aftershocks of much bigger events; no gigantic earthquake (5×10^{28} or more) has been a 'tsunami earthquake'. This may be a reflection of the fact that the yield stresses inside sedimentary material are smaller than in hard rock. However, the possibility cannot be totally discarded of a major rupture occurring inside such a structure. These events are difficult to recognize from their seismic waves alone, since the excitation of Rayleigh waves is practically unchanged in sediments. Clearly, their rapid identification still presents a challenge to the seismological community.
- Non-double couple sources located in hard rock are in principle benign, in that their relative efficiency at exciting Rayleigh waves and tsunamis is comparable to that of regular thrust faulting. However, these sources are believed to correspond to events (submarine volcanic eruptions, landslides) which are by definition very shallow; once placed in sedimentary layers, these sources can under certain geometries feature enhanced tsunami excitation similar to that of regular thrust faulting.
- Finally, lateral depth heterogeneity along the path of tsunami waves can result in focusing and defocusing effects which can reach a factor of 3 for the amplitude of the tsunami. The principle of seismic reciprocity can be used to produce, for a given receiving shore, inverse diagrams featuring seismic regions whose tsunamis will be focused or defocused towards that shoreline (Woods and Okal, 1987).

Acknowledgements

My interest in tsunami danger in the Pacific Basin has evolved from many years of stimulating collaboration with Jacques Talandier. Some surface wave computations

in the present paper were performed using codes originally written by David Harkrider and Robert Herrmann. I thank Mark Woods for collaboration on the ray-tracing of tsunami waves. Publication of this paper was supported by NSF.

References

Abe, K.: 1973, Tsunami and mechanism of great earthquakes, *Phys. Earth Planet. Inter.* **7**, 143–153.

Abe, K.: 1979, Size of great earthquakes of 1837–1974 inferred from tsunami data, *J. Geophys. Res.* **84**, 1561–1568.

Abe, K.: 1983, A new scale of tsunami magnitude, M_t, in K. Iida and T. Iwasaki (eds), *Tsunamis – Their Science and Engineering*, Terrapub, Tokyo, pp. 91–101.

Aki, K. and Richards, P. G.: 1980, *Quantitative Seismology*, W. H. Freeman, San Francisco.

Ben-Menahem, A. and Singh, S. J.: 1981, *Seismic Waves and Sources*, Springer, New York, 1981.

Ben-Menahem, A. and Rosenman, M.: 1972, Amplitude patterns of tsunami waves from submarine earthquakes, *J. Geophys. Res.* **77**, 3097–3128.

Comer, R. P.: 1980, Tsunami height and earthquake magnitude: theoretical basis of an empirical relation, *Geophys. Res. Lett.* **7**, 445–448.

Comer, R. P.: 1982, Tsunami generation: validity of decoupling the ocean from the solid Earth, *Eos, Trans. Amer. Geophys. Un.* **63**, 376 [abstract].

Eissler, H. K. and Kanamori, H.: 1987, A single-force model for the 1975 Kalapana, Hawaii, earthquake, *J. Geophys. Res.* **92**, 4827–4836.

Fukao, Y.: 1979, Tsunami earthquakes and subduction processes near deep-sea trenches, *J. Geophys. Res.* **84**, 2303–2314.

Geller, R. J.: 1976, Scaling relations for earthquake source parameters and magnitudes, *Bull. Seismol. Soc. Amer.* **66**, 1501–1523.

Gilbert, F.: 1970, Excitation of the normal modes of the Earth by earthquake sources, *Geophys. J. Res. Astr. Soc.* **22**, 223–226.

Gilbert, F. and Dziewonski, A. M.: 1975, An application of normal mode theory to the retrieval of structural parameters and source mechanisms from seismic spectra, *Phil. Trans. Roy. Soc. London* **278A**, 187–269.

Harkrider, D. G. and Press, F.: 1967, The Krakatoa air-sea waves: an example of pulse propagation in coupled systems, *Geophys. J. Roy. Astr. Soc.* **13**, 139–159.

Hwang, L.-S. and Lin, A.: 1970, Experimental investigation of wave run-up under the influence of local geometry, in W. Adams (ed.), *Tsunamis in the Pacific Ocean*, East-West Center Press, Honolulu, pp. 407–426.

Iida, K., Suzuki, T., Inagaki, K., and Hasegawa, K.: 1983, Finite element method for tsunami wave propagation in the Tokai district, in K. Iida and T. Iwasaki (eds.), *Tsunamis: Their Science and Engineering*, Terrapub, Tokyo, 1983, pp. 293–301.

Kanamori, H.: 1970, The Alaska earthquake of 1964: Radiation of long-period surface waves and source mechanism, *J. Geophys. Res.* **75**, 5029–5040.

Kanamori, H.: 1972, Mechanism of tsunami earthquakes, *Phys. Earth Planet. Inter.* **6**, 346–359.

Kanamori, H.: 1985, Non-double couple seismic source, *Proc. XXIIIrd Gen. Assemb. Intl. Assoc. Seismol. Phys. Earth Inter., Tokyo, 1985*, p. 425, [abstract].

Kanamori, H. and Cipar, J. J.: 1974, Focal process of the great Chilean earthquake, May 22, 1960, *Phys. Earth Planet. Inter.* **9**, 138–136.

Kanamori, H. and Given, J. W.: 1982, Analysis of long-period seismic waves excited by the May 18, 1980 eruption of Mount St. Helens – A terrestrial monopole?, *J. Geophys. Res.* **87**, 5422–5432.

Kanamori, H. and Stewart, G. S.: 1976, Mode of the strain release along the Gibbs Fracture Zone, Mid-Atlantic Ridge, *Phys. Earth Planet. Inter.* **11**, 312–332.

Kanamori, H., Given, J. W., and Lay, T.: 1984, Analysis of seismic body waves excited by the Mount St. Helens eruption of May 18, 1980, *J. Geophys. Res.* **89**, 1856–1866.

Kanamori, H., Ekström, G., Dziewonski, A. M., and Barker, J. S.: 1986, An anomalous seismic event near Tori-Shima, Japan: a possible magma injection event, *Eos, Trans. Amer. Geophys. Un.* **67**, 1117 [abstract].

Kienle, J., Kowalik, Z., Murty, T. S.: 1987, Tsunamis generated by eruptions from Mount St. Augustine, *Science* **236**, 1442–1447.

Lynnes, C. S. and Ruff, L. J.: 1985, Source process and tectonic implications of the great 1975 North Atlantic earthquake, *Geophys. J. Roy. astr. Soc.* **82**, 497–510.

Okal, E. A.: 1978, A physical classification of the Earth's spheroidal modes, *J. Phys. Earth* **26**, 75–103.

Okal, E. A.: 1982a, Mode-wave equivalence and other asymptotic problems in tsunami theory, *Phys. Earth Planet. Inter.* **30**, 1–11.

Okal, E. A.: 1982b, Higher moment excitation of normal modes and surface waves, *J. Phys. Earth* **30**, 1–31.

Okal, E. A. and Talandier, J.: 1987, M_m: Theory of a variable-period mantle magnitude, *Geophys. Res. Lett.* **14**, 836–839.

Raichlen, F., Lepelletier, T. G., and Tam, C. K.: 1983, The excitation of harbors by tsunamis, in K. Iida and T. Iwasaki (eds.), *Tsunamis: Their Science and Engineering*, Terrapub, Tokyo, pp. 359–385.

Satake, K.: 1988, Effects of bathymetry on tsunami propagation: Application of ray-tracing to tsunamis, *Pure Appl. Geoph.* **126**, 27–36.

Shimazaki, K.: 1975, Nemuro-Oki earthquake of June 17, 1973: A lithospheric rebound at the upper half of the interface, *Phys. Earth Planet. Inter.* **9**, 315–327.

Silver, P. G. and Jordan, T. H.: 1983, Total moment spectra of fourteen large earthquakes, *J. Geophys. Res.* **88**, 3273–3293.

Sommerfeld, A.: 1964, *Optics*, Academic Press, New York.

Spudich, P. K. P. and Orcutt, J. A.: 1980, Petrology and porosity of an oceanic crustal site: results from waveform modeling of seismic refraction data, *J. Geophys. Res.* **85**, 1409–1433.

Talandier, J. and Okal, E. A.: 1979, Human perception of *T* waves: the June 22, 1977 Tonga earthquake felt on Tahiti, *Bull. Seismol. Soc. Amer.* **69**, 1475–1486.

Talandier, J., Reymond, D., and Okal, E. A.: 1987, M_m: Use of a variable-period mantle magnitude for the rapid one-station estimation of teleseismic moments, *Geophys. Res. Lett.* **14**, 840–843.

Ward, S. N.: 1980, Relationships of tsunami generation and an earthquake source, *J. Phys. Earth* **28**, 441–474.

Ward, S. N.: 1981, On tsunami nucleation: I. A point source, *J. Geophys. Res.* **86**, 7895–7900.

Ward, S. N.: 1982a, On tsunami nucleation: II. An instantaneous modulated line source, *Phys. Earth Planet Inter.* **27**, 273–285.

Ward, S. N.: 1982b, Earthquake mechanism and tsunami generation: the Kurile Islands event of October 13, 1963, *Bull. Seismol. Soc. Amer.* **72**, 759–777.

Woods, M. T. and Okal, E. A.: 1987, Effect of variable bathymetry on the amplitude of teleseismic tsunamis: a ray-tracing experiment, *Geophys. Res. Lett.* **14**, 765–768.